LWT - Food Science and Technology 44 (2011) 1786–1792

Contents lists available at ScienceDirect

LWT - Food Science and Technology

journal homepage: www.elsevier.com/locate/lwt

Drying of chitosan in a spouted bed: The influences of temperature and equipment geometry in powder quality

Guilherme L. Dotto, Vanderlei C. Souza, Luiz A.A. Pinto*

Unit Operation Laboratory, School of Chemistry and Food, Federal University of Rio Grande – FURG, 475 Engenheiro Alfredo Huch Street, 96201-900 Rio Grande, RS, Brazil

ARTICLE INFO

Article history:
Received 9 July 2010
Received in revised form
12 March 2011
Accepted 16 March 2011

Keywords:
Color
Deacetylation degree
Molecular weight
Particle size
Temperature

ABSTRACT

The influence of temperature and spouted bed geometry in drying chitosan with relation to powder quality (molecular weight, deacetylation degree, particle size, color) and operation characteristics (product recovery and mass accumulated) were investigated. Chitosan paste was obtained from shrimp wastes and dried in a spouted bed (slot-rectangular and conical-cylindrical geometries) with different inlet air temperatures (90, 100 and 110 °C). Thermogravimetric curves, infra-red analysis and scanning electron microscopy were carried out in order to verify powder quality. Chitosan paste used in drying experiments showed solid content 4%, molecular weight 140 kDa and deacetylation degree 85%. In all drying experiments deacetylation degree was not modified and final moisture content was in the commercial range (10%). Temperature increase caused an increase in molecular weight, powder darkening and increased particle size. The best powder quality was obtained in slot-rectangular spouted bed at 90 °C. In this condition product recovery was 65%, accumulated mass was 20% and the powder presented faint yellow coloration, high thermal stability and porous heterogeneous surface.

1. Introduction

Chitosan; a linear polysaccharide consisting of (1, 4)-linked 2-amino-deoxy-b-D-glucan, is a deacetylated derivative of chitin, which is the second most abundant polysaccharide found in nature after cellulose (Aider, 2010). Chitosan is the only pseudo natural cationic polymer and thus, it has many applications that due its unique character. The main applications of chitosan are food and beverages, agriculture, water and waste treatment, cosmetics and bio-pharmaceutics. Molecular weight, deacetylation degree, color, particle size are important characteristics in relation to the application range of chitosan (Rinaudo, 2006).

The drying operation is important in chitosan production in order to guarantee necessary moisture content for product storage, without causing alterations in the material. In drying of chitosan, temperature is a fundamental parameter, because, chitosan is composed mainly of carbohydrate monomer units capable of undergoing polymerization during the operation. Studies have been carried out on chitosan drying in tray drier (Batista, Rosa, & Pinto, 2007), spray drier (He, Davis & Illum, 1999; Muzzarelli, Stanic, Gobbic, Tosib, & Muzzarelli, 2004), oven drying and infra-red drying (Srinivasa, Ramesh, Kumar, & Tharanathan, 2004), sun drying (Youn, No, & Prinyawiwatkul, 2009), however, in literature, spouted bed drying of chitosan under different conditions has not been studied.

Spouted bed drying of liquids and pastes with inert bodies, is an emerging technology (Pallai, Szentmarjay, & Mujumdar, 2006, chapter 14), and has been presented as an alternative to spray drying, in an attempt to obtain powdered products with the same quality, at low cost (Shuhama, Aguiar, Oliveira, & Freitas, 2003; Cordeiro & Oliveira, 2005; Benali & Amazouz, 2006; Wachiraphansakul & Devahastin, 2007; Passos, Trindade, D'angelo & Cardoso, 2008; Oliveira, Rosa, Moraes, & Pinto, 2008; Souza & Oliveira, 2009). In these driers, some characteristics contribute to drying performance such as good solids mixing coupled with satisfactory gas-particle contact, which promote high rates of heat and mass transfer to the system. In spouted bed driers, the product properties and drier performance are dependent of the operating conditions and of the system configuration (Pallai et al., 2006; Passos, Trindade, d'Angelo, & Cardoso, 2008; Souza & Oliveira, 2009). Spouting is usually carried out in cylindrical vessels equipped with a diverging conical base, however, there are many variants. Spouted beds present three different geometries: cylindrical, conical-cylindrical (including completely conical as a special case), and slot-rectangular. The different geometries have unique characteristics, thus influencing in the process and powder characteristics (Cui & Grace, 2008).

* Corresponding author. Tel.: +55 53 3233 8648; fax: +55 53 3233 8745.
E-mail address: dqmpinto@furg.br (L.A.A. Pinto).

0023-6438
doi:10.1016/j.lwt.2011.03.019

Nomenclature

a	Chromaticity from green to red.
$A_{C=O}$	Absorbance of C═O group.
A_{-OH}	Absorbance of −OH group.
b	Chromaticity from blue to yellow.
D_{mi}	Arithmetic average diameter between two screens (m).
D_P	Particle size (μm).
D_{sauter}	Average diameter of Sauter defined in Eq. (5), (m).
H_{ab}	Hue angle defined in Eq. (4), (°).
K	Constant for chitosan in system of acetic acid/sodium chloride at 25 °C (mL g^{-1}).
m_c	Collected mass in the cyclone (g).
m_{FB}	Total bed mass in the end of operation (g).
m_I	Total solid mass introduced into the drier (g).
m_{IB}	Total bed mass in the begin of operation (g).
Mw	Molecular weight defined in Eq. (3), (kDa).
U_F	Final moisture content (g 100 g^{-1}).
U_{FB}	Final moisture content of powder accumulated in the bed (g 100 g^{-1}).
α	Constant for chitosan in system of acetic acid/sodium chloride at 25 °C (dimensionless).
η	Intrinsic viscosity (mL g^{-1}).
%DD	Deacetylation degree defined in Eq. (6), (%).
A_C	Mass accumulated in the bed defined in Eq. (1) (g 100 g^{-1}).
R	Product recovery defined in Eq. (2) (g 100 g^{-1}).

In order to guarantee commercial moisture content for product storage, without causing alterations in the material, chitosan was dried in a spouted bed. The influences of inlet air temperature and equipment geometry in respect to chitosan quality aspects (molecular weight, deacetylation degree, particle size and color) and operation characteristics (product recovery and mass accumulated) were investigated. Thermogravimetric curves (TG and DTG), infra-red analysis (FT-IR) and scanning electronic microscopy (SEM) were carried out to verify powder quality.

2. Material and methods

2.1. Raw material

Raw material used for chitosan production was shrimp (*Farfantepenaeus brasiliensis*) waste from fishery industries. Shrimp wastes were submitted to demineralization, deproteinization and deodorization, obtaining chitin. Chitosan paste was obtained from alkaline deacetylation of chitin followed by purification (Weska, Moura, Batista, Rizzi, & Pinto, 2007).

2.2. Drying equipment

Chitosan paste was dried in slot-rectangular and conical-cylindrical spouted beds. The conical-cylindrical cell was constituted of a stainless steel cylindrical column with cones of glass. The conical base with enclosed angle of 60° had a height of 0.15 m and the cylindrical column had diameter and height of 0.175 and 0.75 m, respectively. The drier had ratio of 1:6 between the column diameter and the air inlet diameter. The slot-rectangular cell was constituted of a triangular base with enclosed angle of 60° and height 0.2 m. The column had a rectangular transversal section (0.07 × 0.3 m) and height 0.5 m. The air inlet diameter had 0.075 m.

In the two geometries, the air was supplied to the system through a radial blower (Weg, NBR7094, Brazil) with power of 6 kW and maximum outflow of 0.1 $m^3\ s^{-1}$. It was heated in a system of three electric resistances of 800 W each. The heat control of the exit air stream was carried out by a temperature controller (Contemp, IDO2B, Brazil). The drying air velocity was measured by orifice meter, and the pressure drop was measured through the stream bed with U tube manometer (measurement range from 0 to 5000 Pa). The temperatures measured were carried out in type K copper-constantan thermocouples. The chitosan dry powder was collected in a lapple cyclone.

The inert particles used in the spouted bed were polyethylene *pellets* (diameter 0.003 m, sphericity 0.7, density 960 kg m^{-3}). The cell was loaded with 2 kg of inert particles.

2.3. Operating conditions

2.3.1. Fluid dynamics of the equipment

In order to determine the air drying velocity in all experiments, fluid dynamic curves were carried out. The drying cell was loaded with polyethylene *pellets*. Later, the system was started, turning on the radial blower to supply air to the system, and also, turning on the electrical heating until the set point temperature was reached. The behavior of the bed was found through the pressure drop for each increase of air velocity. Maximum pressure drop and the minimum spouting velocity (point where the bed collapse occurred) were found. The fluid dynamics was carried out in all temperatures used (90, 100 and 110 °C).

2.3.2. Drying of chitosan

In each geometry, chitosan was dried in three inlet air temperatures (90, 100 and 110 °C), and air velocity used in the experiments was 100% over minimum spouting velocity, as recommended by Mathur and Epstein (1974) for pastes drying. When a steady velocity regime was established, the feeding system was set in motion and the chitosan paste with solid content of 4 g 100 g^{-1} (wet basis) was fed (0.18 kg paste kg $inert^{-1}\ h^{-1}$) into the cell, through atomization with peristaltic pump and air compressed at pressure of 10^5 Pa gauge. Spouted bed chitosan drying occurred by fluid-particle contact, and also by friction between inert particles caused by the high rate of circulation of the inert in the spouted bed interior. Dried chitosan in powder form was transported pneumatically by the drying air stream and collected in a cyclone. The dry and wet bulb temperatures of air drying were measured. The drying spouted bed experiments were carried out in 3 h, later the dried product was analyzed. Dryer performance was evaluated through determination of the accumulated mass in the bed and product recovery. Accumulated mass and product recovery were estimated by mass balance in the drier using Eqs. 1 and 2:

$$A_C = \frac{(m_{FB} - m_{IB})(1 - U_{FB})}{m_I} \times 100 \quad (1)$$

$$R = \frac{m_c(1 - U_F)}{m_I} \times 100 \quad (2)$$

where, A_C is the mass accumulated in the bed (g 100 g^{-1}), R is product recovery (g 100 g^{-1}), m_{FB} and m_{IB} are total bed mass in the end and in the begin of operation, respectively, U_{FB} is final moisture content of the powder accumulated in the bed (g 100 g^{-1}), U_F is final moisture content of powder (g 100 g^{-1}), m_I and m_C are total solid mass introduced into the drier and collected in the cyclone, respectively.

2.4. Paste and powder characterization

Chitosan paste was characterized according to centesimal chemical composition (A.O.A.C., 1995), molecular weight and deacetylation degree.

Chitosan powder was characterized according to molecular weight, deacetylation degree, color and particle size. In the best drying condition, TG and DTG curves, FT-IR analysis and SEM were carried out to verify the powder quality.

2.4.1. Molecular weight determination

Chitosan molecular weight was determined by viscosimetric method (Cannon-Fenske capillary viscosimeter, model Schott Gerate, GMBH-D65719, Germany). Reduced viscosity was determined by Huggins equation, and converted into molecular weight through Mark-Houwink-Sakurada equation (Eq. (3)), using $K = 1.81 \times 10^{-3}$ mL g^{-1} and $\alpha = 0.93$ (Weska et al., 2007).

$$[\eta] = K M_w^{\alpha} \quad (3)$$

where, η is intrinsic viscosity (mL g^{-1}) and Mw is chitosan molecular weight (kDa).

2.4.2. Color analysis

Chitosan color was found through Minolta system (CR-300, Minolta Corporation, USA). Color was measured from three-dimensional color diagram (L-a-b), and numerical values (a-b) were converted in Hue angle according Eq. (4) (Srinivasa et al., 2004):

$$H_{ab} = \tan^{-1}(a/b) \quad (4)$$

where, H_{ab} is Hue angle (°), "a" is chromaticity from green to red and "b" is chromaticity from blue to yellow.

2.4.3. Particle size determination

Powder grain-size analysis was carried out in standardized mesh screen. The average diameter was calculated by definition of Sauter (Eq. (5)):

$$\overline{D}_{Sauter} = \frac{1}{\sum \frac{\Delta X_i}{D_{mi}}} \quad (5)$$

where, D_{Sauter} is the average diameter of Sauter (m), ΔX_i is the weight fraction of particles size D_{mi} (%) and D_{mi} is the arithmetic average diameter between two screens (m).

2.4.4. TG and DTG curves

Thermogravimetric (TG and DTG) curves were obtained in a thermobalance (TA Instruments, DSC 2010, USA), with a heating rate 10 °C min^{-1} under modified atmosphere through N_2 (50 mL min^{-1}), the amount of samples used was in the range of 1–5 mg in platinum pan in the temperature range of 20–800 °C (Yoshida, Bastos, & Franco, 2010).

2.4.5. SEM studies

Chitosan powder was characterized by scanning electron microscopy, SEM (Jeol, JSM- 6060, Japan) (Yen & Mau, 2007).

2.4.6. FT-IR analysis

Chitosan characteristic bands and deacetylation degree were verified through FT-IR analysis. Chitosan powder was macerated and submitted to the spectroscopic determination in the region of the infra-red ray (Prestige 21, 210045, Japan), using the technique of diffuse reflectance in potassium bromide (Yen & Mau, 2007). Deacetylation degree was determined according to Eq.(6) (Cervera et al., 2004):

$$\%DD = 87.8 - [3(A_{C=O}/A_{-OH})] \quad (6)$$

where, %DD is chitosan deacetylation degree (%), $A_{C=O}$ is absorbance of C=O group and A_{-OH} is absorbance of −OH group.

2.5. Statistical analysis

The responses considered in the drying experiments were compared statistically using Tukey test by the software Statistica 6.0 (Statsoft, USA), with difference significance level of 95% ($p \leq 0.05$).

3. Results and discussion

3.1. Chitosan paste characterization

Chitosan paste obtained showed moisture content 94 ± 0.1 g 100 g^{-1} (wet basis), ashes 0.04 ± 0.01 g 100 g^{-1}, N-chitosan 5 ± 1.0 g 100 g^{-1}, molecular weight 140 ± 2 kDa and %DD 85 ± 1%. For drying experiments the chitosan paste was diluted until 4 g 100 g^{-1} solids.

3.2. Drying operation

Through pressure drop velocity curves, the air drying velocity used in the experiments to guarantee spouted stability was determined. The pressure drop velocity curves obtained were similar to the generic pressure drop velocity curve showed by Mathur and Epstein (1974). In slot-rectangular geometry minimum spouting, the velocities found were 0.88 m s^{-1}, 0.87 m s^{-1} and 0.85 m s^{-1} for temperatures of 90, 100 and 110 °C, respectively. In conical-cylindrical geometry minimum spouting, the velocities were 0.62 m s^{-1}, 0.61 m s^{-1}, 0.60 m s^{-1}, for temperatures of 90, 100 and 110 °C, respectively.

Chitosan paste was fed into the bed. In spouted bed drying, two fundamental parameters are important in order to guarantee quality aspects of product and stable spouted regime, these are residence time and outlet air drying temperature (Pallai et al., 2006). Residence time is important in the drying, because, it determines the relation between materials degradation with drying conditions (Adamiec, Kaminski, Markowski, & Strumillo, 1995, chapter 25). The outlet air drying temperature is a key control variable to obtain the optimal product quality (Benali & Amazouz, 2006). In this work, residence time was considered since the beginning of the operation until the equipment enters into the regime. The stable spouted regime is found when the outlet of air drying temperature becomes constant. Fig. 1 shows outlet air drying temperature for both geometries in all inlet air temperatures.

In Fig. 1 it can be observed that residence time of chitosan paste in the bed was approximately 15 min in all experiments. The residence time values obtained in this work were in the range with those found by Tacon and Freitas (2007), from 12.2 to 17.7 min, in spouted bed drying of pastes. The outlet air drying temperatures had a similar behavior in both geometries (Fig. 1). An increase in inlet air temperature from 90 °C to 100 °C caused an increase in outlet air temperature from 72 ± 1 °C to 84 ± 1 °C, and a new increase in inlet air temperature to 110 °C increased outlet air temperature to 91 ± 1 °C. Chitosan is a carbohydrate and is largely affected by temperature, being that outlet air drying temperature higher than 80 °C is not appropriate, because its polymerization may occur. Therefore, the experiments with inlet air drying temperature of 100 °C and 110 °C do not assure chitosan quality.

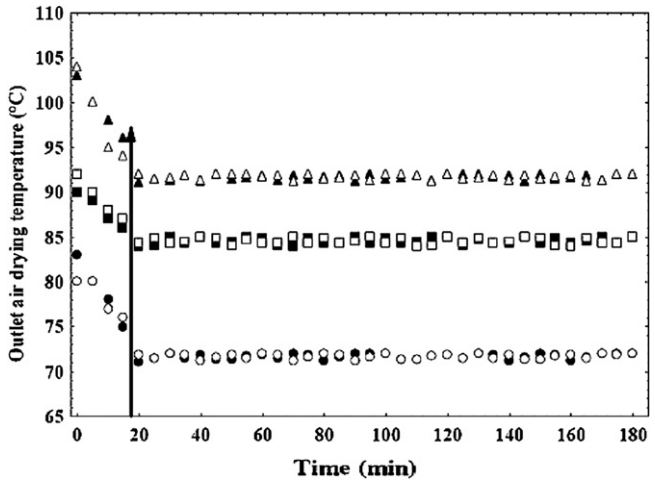

Fig. 1. Outlet air drying temperature in both geometries.Conical-cylindrical spouted bed: (○) inlet air drying temperature 90 °C; (□) inlet air drying temperature 100 °C; (Δ) inlet air drying temperature 110 °C. Slot-rectangular spouted bed: (●) inlet air drying temperature 90 °C; (■) inlet air drying temperature 100 °C; (▲) inlet air drying temperature 110 °C.

3.3. Influence of temperature and geometry in operation characteristics

Table 1 shows the influence of temperature and geometry in accumulated mass (A_C) and product recovery (R).

In Table 1 it can be observed that the temperature increase caused an increase in accumulated mass and decrease in product recovery ($p \leq 0.05$), in addition, it can be observed that conical-cylindrical spouted bed showed higher values of accumulated mass and lower values of product recovery ($p \leq 0.05$).

The dependence of product recovery and accumulated mass in relation to temperature occurred because polyethylene inert can present modifications, because their melting point is 130 °C. So, the adhesion forces in the bed are increased, harming the film break and powder drag, and increasing the accumulated mass and decreasing product recovery.

In relation to geometry influence, the slot-rectangular spouted bed showed higher values of product recovery and lower values of accumulated mass. This occurred because the higher air drying velocity in slot-rectangular spouted bed caused increase in the particle motion inside the bed, increasing the attrition effect, contributing to the removal of the dried product from the spouted bed dryer. Similar behavior was obtained by Souza and Oliveira (2009) in drying of herbal extract in a draft-tube spouted bed.

The product recovery and accumulated mass found in this work were similar to that found by other researchers (Passos et al., 2008; Souza & Oliveira, 2009). Thus the slot-rectangular spouted bed with inlet air drying temperature 90 °C was more appropriate for obtaining higher values of product recovery and lower accumulated mass values.

Table 1
Influence of temperature and geometry in operation characteristics.

Operation characteristics	Conical-cylindrical spouted bed*			Slot-rectangular spouted bed*		
	90 °C	100 °C	110 °C	90 °C	100 °C	110 °C
R (g 100 g^{-1})	48 ± 1^{a}	40 ± 1^{b}	23 ± 1^{c}	65 ± 3^{d}	54 ± 1^{e}	29 ± 1^{f}
A_C (g 100 g^{-1})	30 ± 1^{a}	42 ± 2^{b}	60 ± 3^{c}	20 ± 1^{d}	35 ± 2^{e}	48 ± 2^{f}

*Mean values ± standard error for three experiments. Equal letters in same line ($p > 0.05$). Different letters in same line ($p \leq 0.05$).
R: product recovery; A_C: mass accumulated in the bed.

3.4. Influence of temperature and geometry in powder quality

The main characteristics in relation to chitosan powder quality are deacetylation degree and molecular weight (Rinaudo, 2006). Other fundamental quality aspects are particle size (Piccin, Vieira, Gonçalves, Dotto, & Pinto, 2009) and color (Srinivasa et al., 2004). These characteristics determine the chitosan application range (Rinaudo, 2006), and can be influenced by drying conditions (Batista et al., 2007; Srinivasa et al., 2004; Youn et al., 2009), so, it is important to determine the best drying condition in the spouted bed in order to obtain commercial moisture content, without modifying the product quality. Table 2 shows influence of temperature and geometry in chitosan powder quality.

In Table 2 it can be observed that in all drying experiments, chitosan deacetylation degree was equal to the initial value, so, temperature and geometry did not affect deacetylation degree ($p > 0.05$). Similar behavior was obtained by Youn et al. (2009) in chitosan sun drying at different times. In this case deacetylation degree was not affected, having a range of 81.91 ± 0.73 to 82.73 ± 0.40%.

The spouted bed geometry did not affect chitosan final moisture content ($p > 0.05$), however, a temperature increase caused a decrease in chitosan final moisture content (Table 2). When temperature is increased, convection heat transfer is facilitated, so, evaporation water rate is increased. In addition, effective diffusivity is increased, increasing water mass transfer rate within the material. Similar behavior was obtained by Wachiraphansakul and Devahastin (2007) in drying of okara in a spouted bed. Passos et al. (2008) found moisture content powder between 3 g 100 g^{-1} and 16 g 100 g^{-1} (w.b.) in drying of black liquor in a spouted bed; in this case, inlet temperatures were 80 °C, 100 °C and 120 °C, showing that powder moisture content depend on inlet air temperature. Although moisture content is dependent of temperature, commercial moisture content (until 10 g 100 g^{-1} w.b.) was obtained in all experiments.

The temperature increase caused an increase in powder particle size ($p \leq 0.05$), and more fine powder was obtained in slot-rectangular geometry (Table 2). This behavior can be explained because in slot-rectangular spouted bed, the air drying velocity was higher and attrition effect was more pronounced, thus finer powder was found. In relation to temperature effect, due to the modifications in

Table 2
Influence of temperature and geometry in chitosan quality.

Chitosan characteristics	Conical-cylindrical spouted bed*			Slot-rectangular spouted bed*		
	90 °C	100 °C	110 °C	90 °C	100 °C	110 °C
Mw (kDa)	147 ± 5^{a}	180 ± 3^{b}	225 ± 7^{c}	145 ± 5^{a}	185 ± 3^{b}	220 ± 5^{c}
%DD (%)	85 ± 1^{a}	85 ± 1^{a}	85 ± 1^{a}	85 ± 1^{a}	85 ± 1^{a}	85 ± 1^{a}
H_{ab} (°)	84.5 ± 1.2^{a}	45.7 ± 1.5^{b}	30.3 ± 1.0^{c}	85.5 ± 1.5^{a}	46.7 ± 2.1^{b}	31.1 ± 2.0^{c}
D_P (μm)	100 ± 10^{a}	150 ± 10^{b}	200 ± 20^{c}	70 ± 5^{d}	100 ± 10^{a}	150 ± 10^{b}
U_F (g 100 g^{-1} w.b.)	8.5 ± 1.0^{a}	6.0 ± 0.5^{b}	4.2 ± 0.3^{c}	8.0 ± 0.7^{a}	6.0 ± 0.4^{b}	4.5 ± 0.3^{c}

*Mean values ± standard error for three analysis. Equal letters in same line ($p > 0.05$). Different letters in same line ($p \leq 0.05$).
Mw: Molecular weight; %DD: Deacetylation degree; H_{ab}: Hue angle; D_p: Particle size; U_F: Final moisture content.

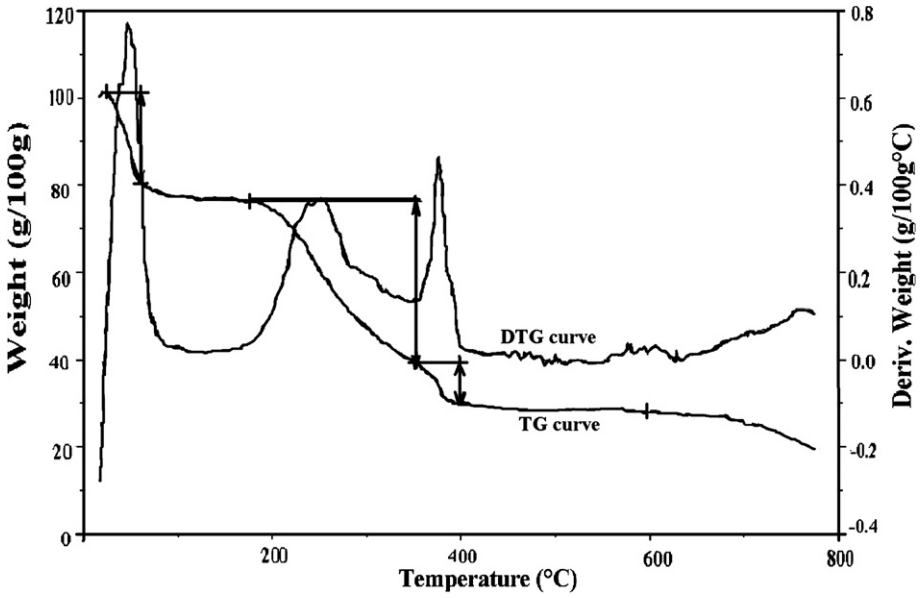

Fig. 2. TG and DTG curves of chitosan powder.

material proprieties with temperature increase, bigger particle sizes were obtained at higher temperature. Similar behavior was obtained by Shuhama et al. (2003), in experimental production of annatto powder in a spouted bed. In this case the temperature increase from 80 °C to 100 °C caused an increase in particle size from 21.6 to 65.5 μm.

Molecular weight and color of chitosan were not affected by the spouted bed geometry ($p > 0.05$), on other hand, temperature increase caused an increase in molecular weight and powder darkening (Table 2). The temperature increase found powder with lower final moisture content and increased outlet air drying temperature, thus chitosan polymerization occurred due to bonding of chitosan chains and consequently the powder darkening. This shows that inlet air drying temperatures of 100 °C and 110 °C cause alterations in chitosan characteristics. Similar behavior was obtained by Srinivasa et al. (2004) in drying of chitosan films in different conditions, they showed that temperature increase from 80 °C to 100 °C caused darkening in chitosan films, and attributed this behavior to Maillard reaction. Wachiraphansakul and Devahastin (2007) in spouted bed drying of okara showed that the temperature increase caused darkening in the powder, increasing oxidation level and decreasing the protein solubility.

Therefore, the best operation condition in spouted bed for chitosan drying was with inlet air drying temperature of 90 °C in a slot-rectangular spouted bed. In this condition, polymerization and darkening of chitosan powder does not occur. In addition, fine

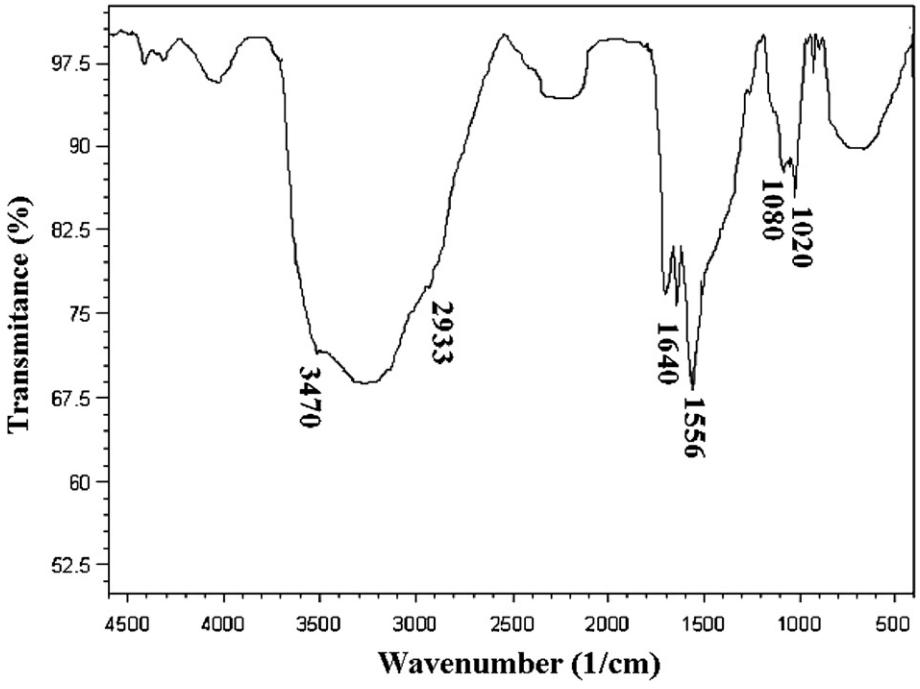

Fig. 3. FT-IR analysis of chitosan powder.

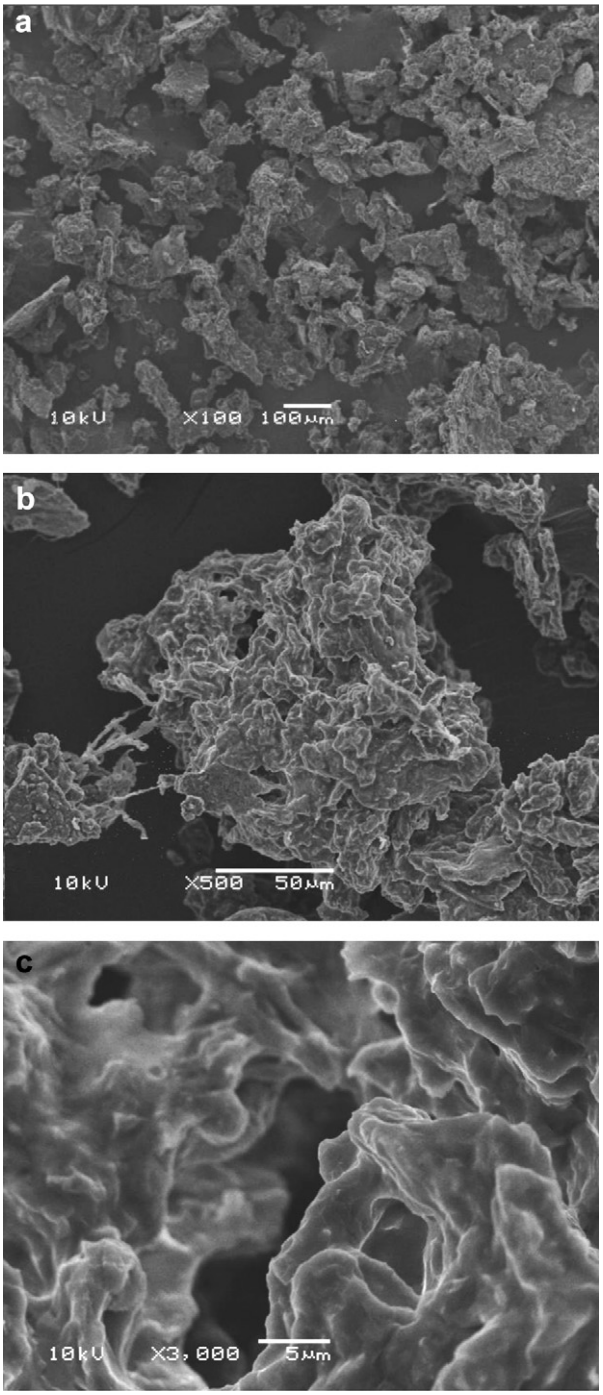

Fig. 4. SEM of chitosan powder: (a) ×100; (b) ×500 and (c) ×3000.

powder with commercial moisture content, deacetylation degree 85% and faint yellow coloration was obtained. Chitosan powder with these characteristics can be used in dye adsorption (Piccin et al., 2009), edible films (Aider, 2010) and membranes (Torres, Aimoli, Beppu, & Frejlich, 2005).

Chitosan powder obtained in the best drying condition was characterized according TG and DTG curves, FT-IR analysis and SEM. Fig. 2 shows TG and DTG curves of chitosan powder.

To determine the temperature ranges in relation to hydration percentages, organic material decomposition and waste, DTG curves were used, related to the first differentiate thermogravimetric curve (Cestari, Vieira, Santos, Mota, & Almeida, 2004). TG and DTG demonstrate that under an atmosphere modified by N_2 (Fig. 2) chitosan mass loss occurred in three steps. The first mass loss step, from about 25 °C to 175 °C concerns the loss of water, which is adsorbed both on the surface and in the pores of the chitosan (Cestari et al., 2004). The decomposition of the chitosan is observed from about 175 °C to 400 °C. A carbonization of material was observed at 400 °C. Thus chitosan powder obtained in spouted bed had high thermal stability.

Fig. 3 shows FT-IR analysis of chitosan powder.

In Fig. 3 chitosan characteristics peaks can be observed. A strong band in 1556 cm^{-1} shows a typical chitosan amino group ($-NH_2$). In 1640 cm^{-1} an axial deformation of C═O (amide band I) can be observed. The weak bands in 1020 cm^{-1} and 1080 cm^{-1} are related to C–N links, and in 2933 cm^{-1} primary amine stretching can be observed. These peaks are involved with functional chitosan amino group. In addition, in 3470 cm^{-1}, hydroxyl groups linked in chitosan structure can be observed. According to Harish Prashanth and Tharanathan (2007), the chitosan amino and hydroxyl groups are the responsible for its unlimited application potential for use in a wide range of faculties.

Fig. 4 shows SEM of chitosan powder obtained from a spouted bed: (a) ×100; (b) ×500 and (c) ×3000.

In Fig. 4(a) it can be observed that chitosan powder obtained in a spouted bed is a fine and homogeneous powder. Fig. 4(b) shows that the chitosan particle obtained had a porous heterogeneous surface. In addition, it can be observed from Fig. 4(c), that porous structure of chitosan powder is mainly constituted of macro porous. These surface characteristics are important in chitosan powder applications, such as, dyes adsorption (Dotto & Pinto, 2011) and active bio-based films (Aider, 2010). Chitosan microspheres prepared by spray drying obtained by He et al. (1999) presented similar characteristics.

4. Conclusion

In this research, the influences of temperature and spouted bed geometry in chitosan drying were studied through the powder quality aspects and operation characteristics. In all temperatures and spouted bed geometries, deacetylation degree was not affected ($p > 0.05$), having in a range of 85 ± 1% and commercial moisture content was obtained. The temperature increase caused an increase in particle size, molecular weight and powder darkening, showing that inlet air drying temperatures of 100 °C and 110 °C cause chitosan polymerization. In addition, temperature increase caused increase in accumulated mass and decrease in product recovery. Slot-rectangular geometry provided finer powder, higher values of product recovery and lower values of accumulated mass.

Thus, the best drying condition for drying chitosan is in a slot-rectangular spouted bed with inlet air drying temperature of 90 °C. In this condition chitosan quality was not affected, product recovery was 65 g 100 g^{-1}, accumulated mass was 20 g 100 g^{-1} and a fine powder with high quality and faint yellow coloration, high thermal stability and a porous heterogeneous surface was obtained.

Acknowledgment

The authors would like to thank CAPES (Brazilian Agency for Improvement of Graduate Personnel) and CNPq (National Council of Science and Technological Development) for the financial support.

References

Adamiec, J., Kaminski, W., Markowski, A. S., & Strumillo, C. (1995). Drying of biotechnological products. In *Handbook of industrial drying*. New York, United States of American: Marcel Dekker.

Aider, M. (2010). Chitosan application for active bio-based films production and potential in the food industry: review. *LWT - Food Science and Technology, 43*, 837–842.

Association of Official Analytical Chemists, AOAC. (1995) (ed. 14).*Official methods of analysis, Vol. 1*.

Batista, L. M., Rosa, C. A., & Pinto, L. A. A. (2007). Diffusive model with variable effetive diffusivity considering shrinkage in thin layer drying of chitosan. *Journal Food Engineering, 81*, 127–132.

Benali, M., & Amazouz, M. (2006). Drying of vegetable starch solutions on inert particles: quality and energy aspects. *Journal of Food Engineering, 74*, 484–489.

Cervera, M. F., Heinamaki, J., Rasanem, M., Maunu, S. L., Karjalainen, M., Acosta, O. M. N., et al. (2004). Solid state characterization of chitosan derived from lobster chitin. *Carbohydrate Polymers, 58*, 401–408.

Cestari, A. R., Vieira, E. F. S., Santos, A. G. P., Mota, J. A., & Almeida, V. P. (2004). Adsorption of anionic dyes on chitosan beads. 1. The influence of the chemical structures of dyes and temperature on the adsorption kinetics. *Journal of Colloid and Interface Science, 280*, 380–386.

Cordeiro, D. S., & Oliveira, W. P. (2005). Technical aspects of the production of dried extract of Maytenus ilicifolia leaves by jet spouted bed drying. *International Journal of Pharmaceutics, 299*, 115–126.

Cui, H., & Grace, J. R. (2008). Spouting of biomass particles: a review. *Bioresource Technology, 99*, 4008–4020.

Dotto, G. L., & Pinto, L. A. A. (2011). Adsorption of food dyes onto chitosan: optimization process and kinetic. *Carbohydrate Polymers, 84*, 231–238.

Harish Prashanth, K. V., & Tharanathan, R. N. (2007). Chitin/chitosan: modifications and their unlimited application potential - an overview. *Trends in Food Science & Technology, 18*, 117–131.

He, P., Davis, S. S., & Illum, L. (1999). Chitosan microspheres prepared by spray drying. *International Journal of Pharmaceutics, 187*, 53–65.

Mathur, K. B., & Epstein, N. (1974). *Spouted beds*. New York: Academic Press.

Muzzarelli, C., Stanic, V., Gobbic, L., Tosib, G., & Muzzarelli, R. A. A. (2004). Spray-drying of solutions containing chitosan together with polyuronans and characterisation of the microspheres. *Carbohydrate Polymers, 57*, 73–82.

Oliveira, E. G., Rosa, G. S., Moraes, M. A., & Pinto, L. A. A. (2008). Phycocyanin content of *Spirulina platensis* dried in spouted bed and thin layer. *Journal of Food Process Engineering, 31*, 34–50.

Pallai, E., Szentmarjay, T., & Mujumdar, A. S. (2006). Spouted bed drying. In *Handbook of industrial drying*. Philadelphia, United States of American: Taylor & Francis Group.

Passos, M. L., Trindade, A. L. G., d'Angelo, J. V. H., & Cardoso, M. (2008). Drying of black liquor in spouted bed of inert particles. *Drying Technology, 22*, 1041–1067.

Piccin, J. S., Vieira, M. L. G., Gonçalves, J., Dotto, G. L., & Pinto, L. A. A. (2009). Adsorption of FD&C red No. 40 by chitosan: isotherms analysis. *Journal of Food Engineering, 95*, 16–20.

Rinaudo, M. (2006). Chitin and chitosan: properties and applications. *Progress Polymers Science, 31*, 603–632.

Shuhama, I. K., Aguiar, M. L., Oliveira, W. P., & Freitas, L. A. P. (2003). Experimental production of annatto powders in spouted bed dryer. *Journal of Food Engineering, 2003*(59), 93–97.

Souza, C. R. F., & Oliveira, W. P. (2009). Drying of herbal extract in a draft-tube spouted bed. *The Canadian Journal of Chemical Engineering, 87*, 279–288.

Srinivasa, P. C., Ramesh, M. N., Kumar, K. R., & Tharanathan, R. N. (2004). Properties of chitosan films prepared under different drying conditions. *Journal of Food Engineering, 63*, 79–85.

Tacon, L. A., & Freitas, L. A. A. (2007). Paste residence time in a spouted bed dryer. III: effect of paste properties and quality interations. *Drying Technology, 25*, 841–852.

Torres, M. A., Aimoli, C. G., Beppu, M., & Frejlich, J. (2005). Chitosan membrane with patterned surface obtained through solution drying. *Colloids and Surfaces A: Physicochem. Eng. Aspects, 268*, 175–179.

Wachiraphansakul, S., & Devahastin, S. (2007). Drying kinetics and quality of okara dried in a jet spouted bed of sorbent particles. *LWT- Food Science and Technology, 40*, 207–219.

Weska, R. F., Moura, J. M., Batista, L. M., Rizzi, J., & Pinto, L. A. A. (2007). Optimization of deacetylation in the production of chitosan from shrimp wastes: use of response surface methodology. *Journal of Food Engineering, 80*, 749–753.

Yen, M. T., & Mau, J. L. (2007). Physico-chemical characterization of fungal chitosan from shiitake stipes. *LWT, 40*, 472–479.

Yoshida, C. M. P., Bastos, C. E. N., & Franco, T. T. (2010). Modeling of potassium sorbate diffusion through chitosan films. *LWT - Food Science and Technology, 43*, 584–589.

Youn, D. K., No, H. K., & Prinyawiwatkul, W. (2009). Physicochemical and functional properties of chitosans affected by sun drying time during decoloration. *LWT - Food Science and Technology, 42*, 1553–1556.